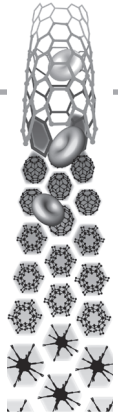

Procoagulant properties of bare and highly PEGylated vinyl-modified silica nanoparticles

Aims: Undesired alterations of the blood clotting balance may follow the intravascular injection of nanotherapeutics/diagnostics. Here, we tested the procoagulant activity of synthetic amorphous silica (SAS) and organically modified silica (ORMOSIL) nanoparticles (NPs) and whether a high-density polyethylene glycol coating minimizes these effects. **Materials & methods:** Hageman factor- and tissue factor-dependent activation of human blood/plasma coagulation, and binding to human monocytes, endothelial cells and platelets were quantified *in vitro* using naked and PEGylated ORMOSIL-NPs. Their effects were compared with those of SAS-NPs, present in many industrial products, and of poly(lactic-co-glycolic acid)- and small unilamellar vesicles-NPs, already approved for use in humans. **Results:** Both SAS-NPs and ORMOSIL-NPS presented a significant procoagulant activity. However, highly PEGylated ORMOSIL-NPs were particularly averse to the interaction with the soluble factors and cellular elements that may lead to intravascular blood coagulation. **Conclusion:** Stealth, highly PEGylated ORMOSIL-NPs with a poor procoagulant activity can be used as starting blocks to design hemocompatible nanomedical-devices.

KEYWORDS: blood coagulation ▪ Hageman factor ▪ HUVEC ▪ liposomes ▪ monocytes ▪ ORMOSIL nanoparticles ▪ PEGylation ▪ platelets ▪ PLGA nanoparticles ▪ synthetic amorphous silica nanoparticles ▪ tissue factor

Regina Tavano[1,2], Daniela Segat[2,3], Elena Reddi[3], Janko Kos[4], Matija Rojnik[4], Petra Kocbek[4], Selma Iratni[5], Dietrich Scheglmann[5], Mario Colucci[6], Iria Maria Rio Echevarria[3,7], Francesco Selvestrel[3,7], Fabrizio Mancin[7*] & Emanuele Papini[†1,2*]

[1]Dipartimento di Scienze Biomediche Sperimentali, Università di Padova, Padova, Italy
[2]Centro di Ricerca Interdipartimentale per le Biotecnologie Innovative, Università di Padova, Padova, Italy
[3]Dipartimento di Biologia, Università di Padova, Padova, Italy
[4]Department of Pharmaceutical Biology, Faculty of Pharmacy, University of Ljubijana, Slovenia
[5]Research & Development Biolitec AG, Winzerlaer Strasse 2, Jena, Germany
[6]Dipartimento di Scienze Biomediche ed Oncologia Umana, Università di Bari, Bari, Italy
[7]Dipartimento di Scienze Chimiche, Università di Padova, Padova, Italy
[†]Author for correspondence:
Tel.: +39 049 827 6301
Fax: +39 049 827 6159
emanuele.papini@unipd.it
**Authors contributed equally*

Nanoparticle (NP)-based imaging and drug delivery have been increasingly proposed in recent years, especially in oncology [1,2]. The administration of various types of drugs through nanosystems is believed to increase their therapeutic efficacy and selectivity. It is assumed that properly targeted NPs can selectively carry packages of active, or activatable, molecules into tumor cells without affecting healthy cells [3].

Nonetheless, the potential toxicity of nanostructures remains a major concern and must be carefully tested to evaluate their biocompatibility [4,5]. In this respect, an immediate risk hampering the injection of NPs into the bloodstream for medical use is the activation of coagulation, a dangerous complication that must be avoided. A foreign material may activate blood coagulation either by direct interaction with clotting factors or through the activation of hemostatically active cells, such as platelets, monocytes and endothelial cells. The first mechanism generally involves the so-called 'contact system' of coagulation, whose factors, by adsorbing to the foreign surface, become activated and trigger the intrinsic pathway of coagulation [6]. This rapid phenomenon may lead to fibrin formation within a few minutes. Alternatively, the foreign material can bind to and activate monocytes, endothelial cells and platelets, leading the synthesis and expression of procoagulant properties, among which tissue factor (TF; i.e., the initiator of the extrinsic pathway of coagulation) is the most powerful, particularly in monocytes [7].

Available evidence suggests that NPs of different nature are able to alter the coagulation balance. Inhaled environmental NPs, such as ultrafine diesel exhaust particles, has been shown to increase vascular thrombosis in animal models [8,9]. Ultrafine carbon black NPs, cationic polystyrene NPs and carbon nanotubes (both single wall and multiwall) were found to be thrombogenic [10,11], possibly owing to their ability to increase platelet aggregation. Quantum dots caused pulmonary thrombosis in animals, very likely owing to their negative superficial charge, which activates the contact coagulation cascade [12]. A strategy used with macroscopic materials to minimize procoagulant effects is to superficially coat them with hemostatically inert molecules or cells. Coating with polyethylene glycol (PEG) has proved to be a successful strategy [12] and, therefore, was also applied to NPs to increase their biocompatibility and to diminish their fast clearance by the macrophages of the reticuloendothelial system [3,13,14].

The development of nanoscale structures that have a core of silica in various combinations with other materials or with targeting molecules and doped with specific drugs, is a main field of investigation in biotechnology and

part of future medicine fsg

nanomedicine [15,16]. Silica, or silicon dioxide, is an abundant natural compound existing in crystalline and noncrystalline (amorphous) form. Amorphous silica is present in nature (e.g., in the diatomaceous earth) and is also produced under controlled conditions by polymerization of silicates and other inorganic precursors (synthetic amorphous silica [SAS]). SAS-NPs are widely used as additives in chemical industry and food manufacturing [17]. In addition, they are cheap, easy to prepare, mechanically resistant, water soluble, relatively chemically inert and they can be easily functionalized (or doped), either at the surface or in the interior. As a consequence, silica particles doped with organic molecules and associated with other nanostructures may have several biomedical applications. Amorphous silica materials can also be obtained by the controlled polymerization of organosilane derivatives (where an organic moiety is covalently linked to the Si atom). NPs made by this organically modified silica (ORMOSIL) retain stability and physicochemical properties similar to those of inorganic SAS. In addition, they have a larger chemical versatility, due to the different organic components that can be selected during synthesis and which are in part also conserved in the final product [18,19]. Organically modified silica has been used for the realization of medical nanodevices useful in therapy, such as photodynamic therapy [20] or optical imaging [21]. With these remarkable qualities, ORMOSIL-NPs are likely to play a prominent place in the next generation of nanovehicles for the delivery of therapeutic/diagnostic agents and, possibly, of more sophisticated nano-objects. Yet, experimental evidence reveals that silica-based nanomaterials are not devoid of detrimental effects. Silica nanocrystals are toxic and responsible for silicosis [22,23]. Also in the case of SAS, protracted (90 days) inhalation studies in animals found variable toxic effects in the lung depending on material type. These were nevertheless less severe compared with those induced by crystalline silica [22]. Although systematic toxicological studies on SAS-NPs have not been performed yet [24], recent data show that they are cytotoxic to different human cell lines [25,26]. In addition, SAS-NPs were shown to induce production of reactive oxygen species in RAW cells [27] and pulmonary inflammation in mice [28]. Intravenous injection of rhodamine-doped silica NPs in mice resulted in liver inflammatory responses for NP size above 100 nm [29]. To the best of our knowledge, no toxicological studies are reported for ORMOSIL-NPs.

The evidence discussed suggests prudence in the use of silica NPs for medical purposes and underlines the need of a better understanding of their interaction with varying biological systems. Despite this, silica NPs and especially organically modified ones, may be conveniently synthesized and modified to eliminate unwanted side effects, thanks to their versatility. Recently, we have developed a one-pot synthesis production of PEGylated ORMOSIL-NPs based on a modification of the method originally proposed by Prasad [30,31], which involves the polymerization of lipophylic organosilane derivatives in the hydrophobic core of detergent micelles. We achieved size-controlled (20–100 nm) production of NPs by the use of an appropriate surfactant (Brij 35) and by tuning the reaction conditions. More importantly, by including a trialkoxysilane modified PEG in the synthesis reaction, we covalently grafted PEG onto the NP surface, obtaining an unprecedented PEG content ranging from 67% (in 20-nm diameter NPs) to 37% (in 50-nm diameter NPs) on weight basis. The initial functional characterization of our highly PEGylated NPs was encouraging; these NPs showed low protein adsorption properties and escaped phagocytosis by human macrophages [32]. Therefore, in this study, we analyzed the ability of non-PEGylated and highly PEGylated ORMOSIL-NPs to induce blood coagulation *in vitro,* either directly or through cell activation. ORMOSIL-NPs were compared with SAS-NPs. Such a comparison also allowed the assessment of the effects of SAS-NPs, which, to our knowledge, have not been investigated with respect to their procoagulant activities. Furthermore, we tested the two main alternative NP classes, which have been shown to be biocompatible and suitable for the use in humans: PLGA (poly[lactic-co-glycolic acid])-NPs [33] and liposomes [34,35], both in non-PEGylated and in PEGylated forms. The ability to avoid capture by resident macrophages of the reticuloendothelial system is now considered the central parameter to screen for NPs' potential application in nanomedicine. Our novel approach is based on the idea that possible activation of procoagulant effects is likely to occur well before blood clearance by phagocytic cells and is therefore the first critical aspect to be considered for evaluating NP biocompatibility. From this point of view, our comparative analysis of the effects of different NP formulations in a bare and PEGylated state on the main actors of blood coagulation/

thrombosis (plasma proteins, monocytes, endothelial cells and platelets) is also aimed at establishing a more comprehensive notion of NP biocompatibility.

Materials & methods

Preparation & characterization of NPs

All NPs were produced using aseptic (filter-sterilized) and endotoxin-free solutions (<0.025 Endotoxin units/ml as measure with *Limulus* test). Organic, modified NPs were prepared as described elsewhere [32]. In brief, Brij 35 (5 mM) was dissolved by stirring in 5 ml of water into a thermostated reaction vessel and, when PEGylated NPs were prepared, a $MPEG_{2000}$ triethoxysilane derivative (3 mM) was added [32]. Subsequently, 150 µl of *n*-butanol and 70 µl of vinyltriethoxysilane were added. The mixture was stirred for 30 min and then 5 µl of aqueous ammonia followed by 10 µl of a 13 mM solution of IR775-Si in DMSO were added [32]. The stirring was continued overnight at constant temperature and then the reaction mixture was filtered through a 0.22 µm membrane filter. Only in the case of PEGylated NPs, Bio-Beads® SM (14.3 mg per mg of Brij 35) were added and the mixture was further stirred for 3 h. The mixture was filtered to remove the beads and the resulting solution was extensively ultrafiltrated with Milli-Q water, using a cellulose membrane with a cut-off size of 10 kD. The mean diameter of the NPs, measured by Dynamic Light Scattering (using a Zetasizer Nano S, Malevern Instruments) was 51 and 45 nm, respectively, for the non-PEGylated and the PEGylated NPs. The zeta-potential values (in phosphate-buffered saline [PBS], pH 7.4) were -6.2 and -4.3 mV, respectively, for the non-PEGylated and the PEGylated NPs. The content of the cyanine dye IR775-Si was 0.03 % (w/w).

Synthetic amorphous silica NPs LUDOX TM-40 were purchased as a 40 wt% suspension in water (Sigma Aldrich). Dynamic light scattering and transmission electron microscope investigations confirm the average diameter of 35 nm. The zeta-potential (in PBS buffer, pH 7.4) was -25.9 mV.

Polyethylene glycol poly(lactic-co-glycolic acid) NPs were prepared by the double emulsion solvent diffusion method under mild experimental conditions as described [36]. Resomers RG® 503 H and RGP® d 50155 (Boehringer) were dissolved in ethyl acetate at a 1:1 (sample 1; 7.5% final PEG) w/w ratio. To prepare fluorescein-labeled NPs, fluorescein was added to the polymer solution (0.25 mg per 1 ml of ethyl acetate) at this stage. After adding deionized water, the primary w/o emulsion was stirred at 7000 rpm (Omni Labteh, Omni Int. Inc.) with simultaneous sonication (ultrasonic bath: 500 W, 30 kHz, UZ 4P Iskra Sentjernej) for 2 min. Then, 5% PVA in aqueous solution was added to the water-in-oil emulsion to form a double emulsion (w/o/w) and stirred for a further 5 min. The NPs were formed after dilution of w/o/w double emulsion with 200 ml of 0.1% PVA in aqueous solution under stirring at 5000 rpm for 5 min. The resulting NPs were recovered by centrifugation at 15000 rpm for 15 min (ultracentrifuge Sorvall RC5C Plus), washed three times with deionized water, placed in liquid nitrogen and freeze-dried (-57°C, 0.090 mbar, 24 h, Christ Beta 1–8K). After resuspension of lyophilized PEG PLGA-NPs in deionized water, the mean diameter was 282 nm, as determined by photon correlation spectroscopy using a Zetasizer 3000 (Malvern Instruments). The polydispersity index was 0.3.

Liposomes with a diameter of approximately 150 nm (small unilamellar vesicle [SUV]-NPs) were produced by extrusion using a mixture of 1.8% (w/v) dipalmitoylphosphatidylcholine (DPPC) and 0.2% (w/v) dipalmitoylphosphatidyl glycerol in 10 mM histidine buffer pH 6.5. PEGylated SUV-NPs were obtained with the same procedure, including 1.6% (w/v) PEG2000 in the mixture. In some experiments, SUV-NPs were doped with 0.1% phycoerythrin (PE) derivative of DPPC. ORMOSIL-NPs and SUV-NPs are stable for months at room temperatures, while PLGA-NPs tend to destabilize in solution after 1 day or longer. NP aggregation state/distribution size was not significantly different in water and in physiologic saline (0.9% NaCl). Endotoxin levels in NPs were determined using the very sensitive *Limulus* test (Sigma aldrich) and was found to be in the range of 0.07 to 0.004 EU per µg of NP.

Blood collection & preparation of platelet-rich & platelet-poor plasma

Venous blood was taken from healthy volunteers and immediately anticoagulated with 3.8% trisodium citrate (9:1 of blood:citrate). In order to minimize *ex vivo* clotting and platelet activation, the first 3 ml of blood were discarded. Platelet-rich plasma (PRP) was obtained by centrifuging blood at 150 g for 10 min, without use of a brake, and contained 290000–300000 platelets/µl. Platelets poor plasma (PPP) was prepared by centrifuging blood at 2000 g for 10 min.

Cell cultures

Human umbilical vein endothelial cells (HUVECs, Promocell) were maintained in medium 200 (M200, Cascade Biologics) supplemented with Low Serum Growth Supplement Kit (LSGS Kit, Cascade Biologics). The cells were maintained at 37°C in a humidified atmosphere containing 5% (v/v) CO_2 and used after two to three passages. The day before the experiment, the cells were detached by trypsinization and 1.5 × 10^6 cells/well were seeded onto a 12-well plate (Falcon).

Monocyte-enriched preparations were isolated from buffy coats of blood by centrifugation over a Ficoll-Hypaque (Amersham Biosciences) step gradient and a subsequent Percoll (Amersham Biosciences) gradient; cells were suspended in RPMI-1640 (GIBCO BRL) supplemented with antibiotic and 2% FCS, and plated onto a 24-well plate (Falcon, 2 × 10^6 cells/well). Residual T and B cells were removed from the monocyte fraction by plastic adherence for 1 h at 37°C. The purity of preparations (percentage of CD14-positive cells) and cell viability (assessed by the trypan blue exclusion test) were both higher than 98%. Unless otherwise specified, cells were kept at 37°C in a humidified atmosphere containing 5% (v/v) CO_2 in RPMI-1640 supplemented with 10% FCS.

Evaluation of hemocompatibility

In vitro hemolysis assay

Fresh citrated blood was mixed at a 1:1 (v/v) ratio with 100 µg/ml of NP suspension in 150 mM NaCl. Blood diluted with distilled water or with PBS was used as negative or positive control, respectively. Samples were incubated at 37°C for 2 h and then centrifuged at 2600 rpm for 7 min. Supernatants were collected and incubated at room temperature for 30 min to allow for hemoglobin oxidation. Oxyhemoglobin concentration was then measured spectrophotometrically at 620 nm.

Whole blood clotting time

A total of 500 µl of fresh citrated blood was mixed 1:1 (v/v) with saline (negative control), 0.002 U/ml ecarin (Sigma, positive control) or different concentrations up to 350 µg/ml of NPs in FACS tubes. Samples were incubated at 37°C in a water bath for 5 min and then calcium chloride was added to obtain a final concentration of 17 mM; the time of clot formation at 37°C was recorded manually using the tilting method.

Plasma clotting time

A total of 100 µl of normal or factor XII-deficient PPP (Haematologic Technologies) was added to 100 µl of NPs at various concentrations in 150 mM NaCl in a 96-well microtiter plate (Sarstedt) and coagulation was started by the addition of 65 µl of 50 mM $CaCl_2$. The plate was incubated at 37°C and the changes in optic density at 405 nm were read every 70 s 100 times. To calculate the mean absorbance at each time point, three wells were averaged per sample. The time required to reach half maximal absorbance increase ($t_{½}$) was calculated and used for statistical analysis. In the same samples, ecarin was added as a positive control. As a negative control, plasma was sometimes coagulated with ecarin (0.1 U/ml), centrifuged to collect serum and incubated as above with NPs.

Induction of TF in monocytes & HUVECs by NPs

Monocytes or HUVECs were incubated at 37°C with lipopolysaccharide (LPS) as a positive control (0.1–3000 EU) or with increasing concentrations of NPs (up to 200 µg/ml). For TF activity assay, cells were incubated for 20 h and then scraped and lysed by triple freezing and thawing. Cell TF activity was determined by a one-stage clotting test as described in [37]. Briefly, cell lysates (100 µl) were mixed with the same volume of PPP and 50 mM $CaCl_2$ in tubes prewarmed at 37°C in a water bath, and the clotting time was determined by visual inspection. Clotting times were converted to TF arbitrary units by comparison with a calibration curve obtained with commercial human thromboplastin (Instrumentation Laboratory); a tenfold dilution of this preparation was assigned a value of 10^5 units of TF. For TF mRNA assay, monocytes or HUVECs were incubated with NPs for 2, 4 or 6 h at 37°C. Cells were then scraped and RNAs were isolated by TRIzol reagent (Invitrogen), according to manufacturer's instructions, and resuspended in 6–8 µl of RNase-free water (Gibco). RNA was quantified by spectrophotometric analysis (NanoDrop® ND-1000 Spectrophotometer, CELBIO) and 300 ng of total RNA was retrotranscripted. First-strand cDNA was prepared by using M-MLV reverse transcriptase (Promega) with random primers (Promega) and used for PCR analysis. Equal amounts of cDNA (5 µl) were amplified by PCR with GoTaq® Flexi DNA Polymerase (Promega), reaction buffer containing $MgCl_2$, PCR nucleotide mix (Promega) and with the following primers: TF: 5′-ggtgggaacaaaagtgaatgtgac-3′

and 5′-tcctttatccacatcaat-3′; GAPDH (internal control): 5′-cggagtcaacggatttggtcgtat-3′ and 5′-agccttctccatggtggtgaagac-3′. The PCR program used the following parameters: initial denaturation for 2 min at 94°C, 30-step PCR cycling; denaturation for 1 min at 94°C, annealing for 1 min at 57°C and 20 s at 72°C; and final extension for 5 min at 72°C. The expected PCR product sizes for TF and GAPDH were 193 and 306 base pairs, respectively.

Binding of NPs to monocytes, platelets & HUVECs

Monocytes and HUVECs, seeded onto 24-well plate were incubated with different concentration of fluorescent PEGylated or non-PEGylated NPs for 20 h and then scraped; alternatively, 10 µl of PRP were incubated with different concentrations of NPs for 10 min at 37°C [38]. Then cells were collected, washed with PBS and resuspended in cold FACS buffer (PBS 1% BSA). Propidium iodide was added to exclude dead cells. NP capture was evaluated by cell fluorescence intensities of the gated populations, measured with a BD FACSCanto II flow cytometer (Becton Dickinson). In other experiments, monocytes (2×10^6 cells/well) and HUVECs (0.3×10^6 cells/well) were seeded onto cover glasses and incubated for 18 h at 37°C, with 50 µg/ml of PEGylated or non-PEGylated fluorescent NPs. Unfixed cells were briefly rinsed in PBS and directly analyzed under a confocal microscope (SP2 Leica).

Induction of cell activation markers in platelets & HUVECs

A total of 10 µl of PRP were incubated with different concentrations of NPs, or with a platelet activator mixture (α-thrombin [THR], 1 U/ml, I-BOP 1 M, ADP 10 µM) in saline (100 µl, final volume) for 10 min at 37°C. Samples were then incubated with irrelevant IgM-PE-conjugated antibody (isotypic control), or with IgM-PE monoclonal antibodies against CD42b (glycoprotein Ib, expressed on the surface of resting and activated platelets) or CD62p (p-selectin, expressed on the surface of activated platelets; Biolegend) for 30 min at 4°C. Samples were then fixed with 0.5% paraformaldehyde and acquired with BD FACSCanto II (Beckton Dickinson). Results were analyzed using BD FACSDiva software, version 6.1.2.

Human umbilical vein endothelial cells were incubated with different concentrations of NPs or with 20 ng/ml of TNF-α (positive control) for 20 h at 37°C. Then, cells were scraped, washed and incubated for 30 min at 4°C with PE-labeled monoclonal antibodies against the following antigens: CD31 (integral membrane protein constitutively expressed on the surface of the endothelial cells), CD106 (VCAM-1, expressed on endothelial cells during inflammation), CD54 (integral membrane protein that plays a role in the cell adhesion) and CD62e (E-selectin expressed on activated endothelium; Biolegend). Finally, cells were washed and suspended in FACS buffer; just before sample acquisition, propidium iodide was added in order to exclude dead cells. Samples were analyzed using BD FACSCanto II.

Platelet aggregation assay

Platelet aggregation responses were monitored by a turbidimetric method using a dual-channel Elvi 840 aggregometer (Elvi Logos). PRP (250 µl) was incubated at 37°C with continuous stirring at 1000 rpm. The degree of platelet aggregation was determined after the addition of 100 µg/ml of different NPs or different concentrations of ADP (as a positive control), and was standardized by assuming that PPP represented 100% light transmission and that PRP represented 0% light transmission. A reduction in turbidity of PRP corresponds to platelet aggregation. PRP was equilibrated at 37°C for 3 min prior to the initiation of each experiment.

Results

Whole blood clotting time in the presence of NPs

Since red blood cell membranes accelerate coagulation reactions, we first determined whether NPs induced red blood cell damage. Blood was incubated with PEGylated and non-PEGylated NPs for 2 h and the release of hemoglobin was measured spectrophotometrically. None of the NPs (200 µg/ml) caused an appreciable release of hemoglobin (not shown).

In order to determine the effect of NPs on whole blood clotting time, fresh blood samples were preincubated for 5 min at 37°C before the addition of $CaCl_2$ to start coagulation. Whole blood clotting time was determined at 37°C by visual inspection (FIGURE 1). Ecarin, a protease from the venom of the viper *Echis carinatus* that directly catalyzes the conversion of prothrombin into α-thrombin, was used as a positive control [39]. Clot formation in untreated blood occurred in approximately 16 min. SAS-NPs shortened clotting time to approximately 3 min, indicating that amorphous SiO_2 particles display a strong procoagulant activity (PCA), even

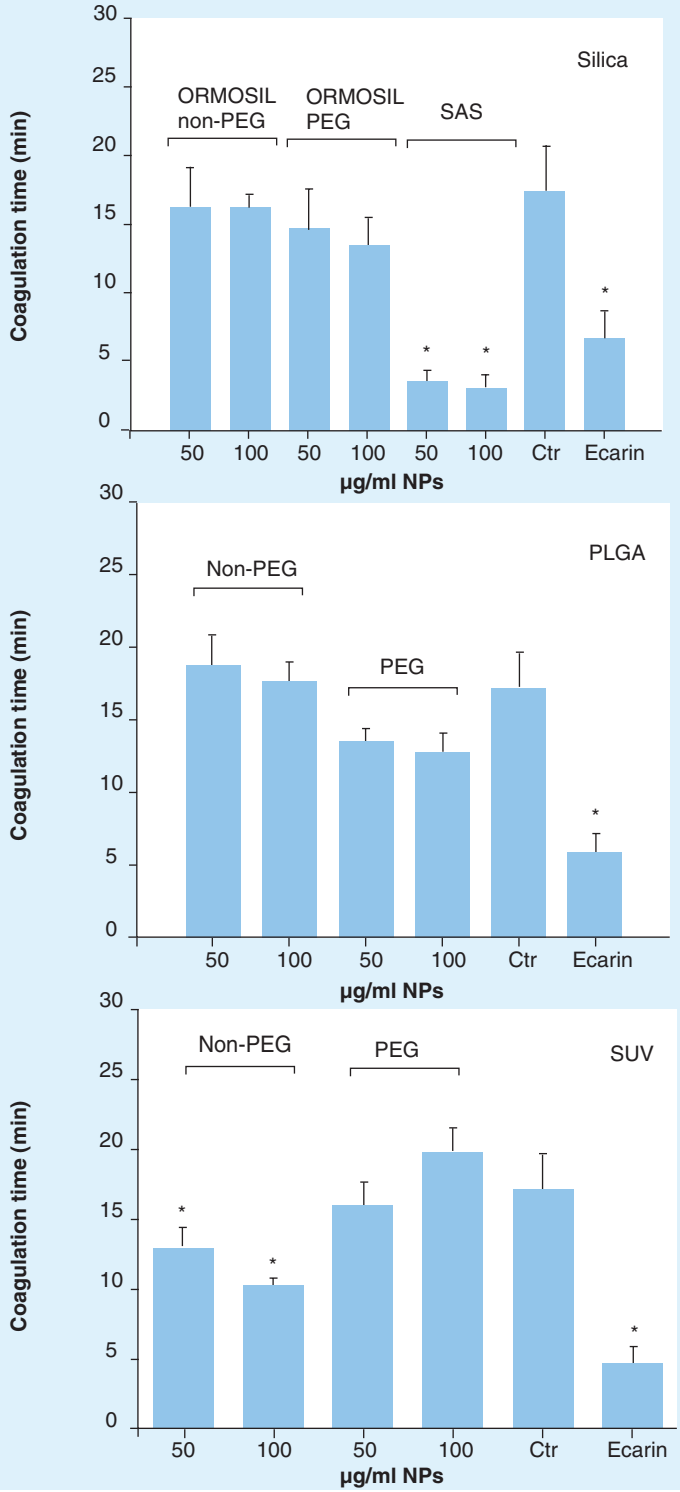

Figure 1. Coagulation time of whole blood in the presence of nanoparticles.
The indicated doses of NPs (SAS, non-PEGylated or PEGylated NPs) were added to whole citrated blood. Coagulation was started by the addition of $CaCl_2$ (17 mM final concentration) and clotting time was chronometrically determined. Positive controls were obtained by adding the prothrombin activator ecarin (0.02 U). Data are the means from a representative experiment out of five, run in triplicate and error bars represent ± SE. Significance of differences with respect to control (no agonist in the presence of Ca^{2+}) clotting times are indicated by * ($p < 0.05$).
Ctr: Control; NP: Nanoparticle; ORMOSIL: Organically modified silica; PEG: Polyethylene glycol; PLGA: Poly(lactic-co-glycolic acid); SAS: Synthetic amorphous silica; SUV: Small unilamellar vesicle; TF: Tissue factor.

more pronounced than that of ecarin (~6 min). ORMOSIL- and PLGA-NPs did not significantly affect blood clotting time, either in the PEGylated or in the non-PEGylated forms. Non-PEGylated SUV-NPs caused a moderate acceleration of the blood coagulation time (~10 min) compared with the controls, while PEGylated SUV-NPs showed no significant activity.

Kinetics of plasma clot formation in the presence of NPs

To better document the NPs' effects on coagulation we evaluated the kinetics of clot formation in plasma using a turbidimetric assay. Fresh PPP was incubated with NPs and fibrin formation was monitored after addition of 17 mM $CaCl_2$ by measuring absorbance increment (405 nm). A left shift of the curve indicates more rapid clot formation. Representative optic density tracings are shown in Figure 2A. SAS markedly accelerated plasma clot formation in agreement with whole blood clotting time assays. Non-PEGylated ORMOSIL-NPs displayed a weak but statistically significant PCA, whereas PEGylated ORMOSIL-NPs had no influence at all on the kinetics of clot formation. Non-PEGylated PLGA-NPs and non-PEGylated SUV-NPs accelerated fibrin formation to a greater extent than bare ORMOSIL-NPs. However, PEGylation also resulted in the complete disappearance of the procoagulant effect of the NPs. Dose–response analysis of plasma coagulation half-time ($t_{½}$) shown in Figure 2B confirmed that SAS were very active, since they were effective at concentrations as low as 1 µg/ml. The same analysis confirmed that bare ORMOSIL-, PLGA- and SUV-NPs are endowed with a moderate coagulant activity, which never resulted, even at high doses (350 µg/ml), in maximal effects achieved with SAS or positive ecarin control. Notably, all PEGylated NPs were devoid of plasma clotting effects. Experiments performed with factor XII depleted plasma showed that coagulation time in the presence of high doses of all type of NPs (350 µg/ml) were strongly delayed ($t_{½}$ > 3 h; data not shown), confirming that plasma clotting occurs via the absorption of Hageman factor (XII) on the surface of naked NPs and the subsequent activation of the contact pathway.

Induction of TF by NPs in monocytes

The assays reported above are suitable to unmask a direct effect of NPs on factor XII-dependent clotting reactions or, in the case of whole blood, an effect resulting from the rapid activation of cells. An alternative mechanism by which

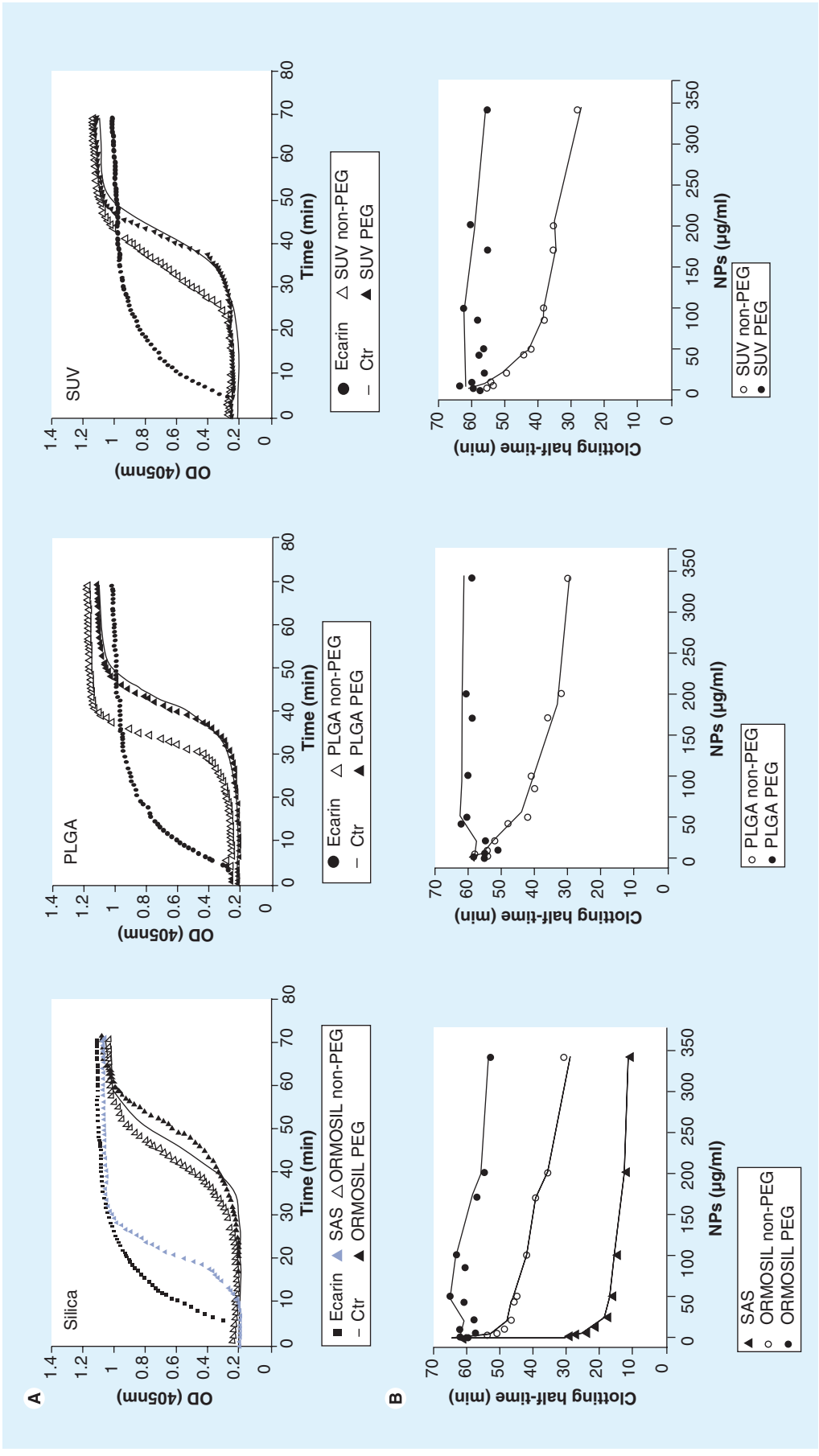

Figure 2. Kinetics of plasma coagulation in the presence of nanoparticles. (A) Representative coagulation kinetics of fresh human platelet-poor plasma (PPP) in the presence of the indicated types of NPs (50 µg/ml) or of maximally active ecarin (0.01 U), as positive controls. NPs were added to microtiter 96-well plates containing 100 µl of PPP in the presence of citrate. After addition of 17 mM $CaCl_2$, the kinetics of plasma coagulation was automatically monitored at different times by reading the absorbance at 405 nm. Ctr corresponds to the coagulation kinetics of PPP in the presence of $CaCl_2$ and without additional stimuli. **(B)** The time corresponding to half maximal coagulation of PPP deduced by kinetics curves as above in the presence of indicated NP concentrations are shown.
Ctr: Control; NP: Nanoparticle; ORMOSIL: Organically modified silica; PEG: Polyethylene glycol; PLGA: Poly(lactic-co-glycolic acid); SAS: Synthetic amorphous silica; SUV: Small unilamellar vesicle.

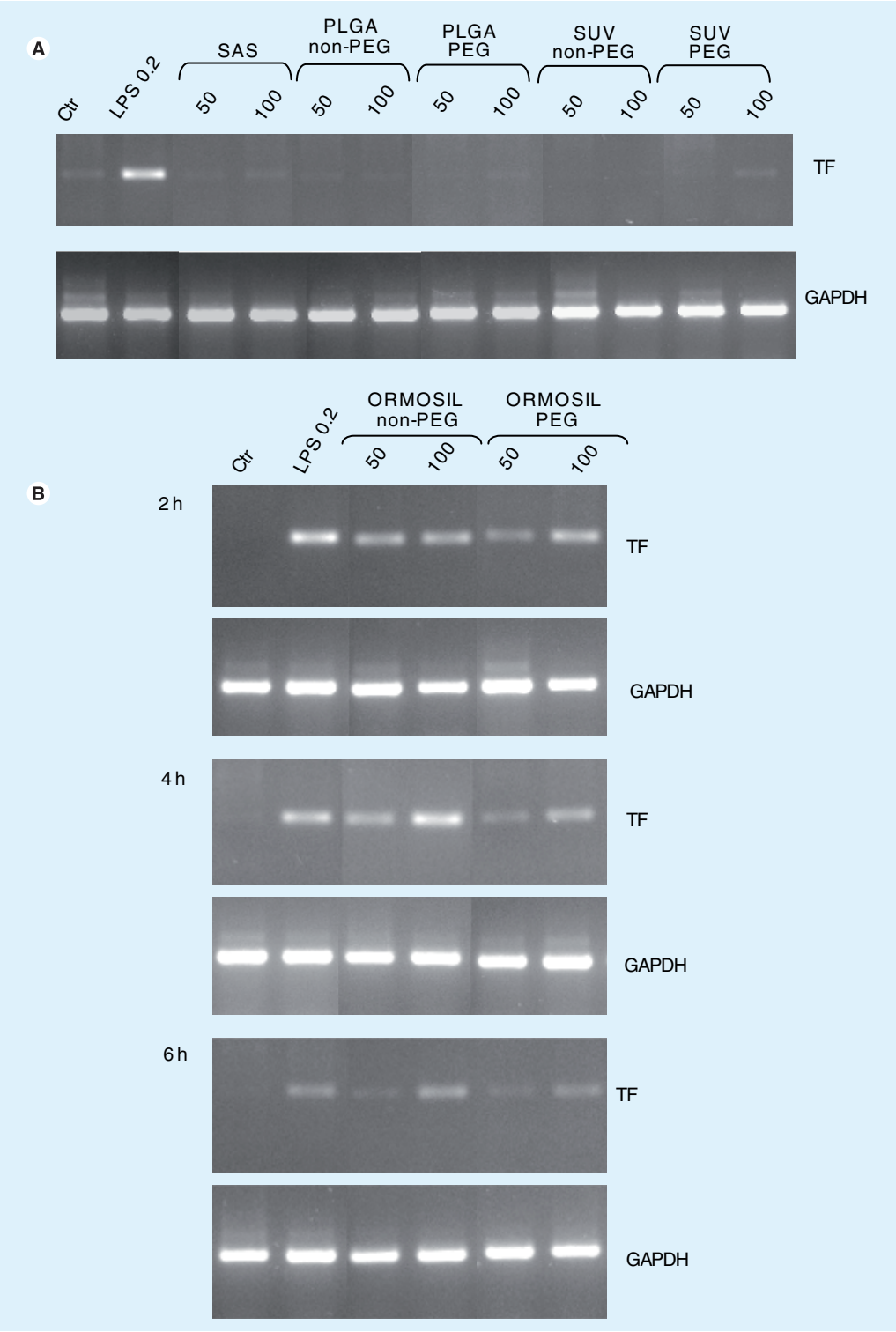

Figure 3. Induction of tissue factor gene transcription by nanoparticles. (A) Different doses of indicated nanoparticles were added to human monocytes isolated from buffy coats. After 4 h of treatment with the monocytes, total RNA was extracted from samples with TRIzol reagent. Equal amount of mRNA was reverse transcribed in cDNA. TF gene transcription was determined by PCR using primers for the TF gene (193 bp) and reporter gene (GAPDH, 306 bp). **(B)** Kinetics of TF gene transcription upon ORMOSIL-nanoparticles treatment in isolated human monocytes. The experiment shown is representative of three experiments conducted with different cell preparations.
Ctr: Control; LPS: Lipopolysaccharide; ORMOSIL: Organically modified silica; PEG: Polyethylene glycol; PLGA: Poly(lactic-co-glycolic acid); SAS: Synthetic amorphous silica; SUV: Small unilamellar vesicle; TF: Tissue factor..

NPs may promote coagulation is through the induction of TF in monocytes and endothelial cells, a phenomenon that takes place in hours and requires the neosynthesis of the TF protein. Therefore, to investigate the possible involvement of cell-derived TF, monocytes and HUVECs were incubated with NPs for several hours, after which TF gene expression and TF activity were determined on cell lysates by real-time (RT)-PCR and a clotting test, respectively.

In monocytes, SAS-NPs as well as non-PEGylated and PEGylated PLGA- and SUV-NPs had virtually no effect on TF gene transcription (Figure 3A). By contrast, non-PEGylated ORMOSIL-NPs induced a clear-cut increase in TF mRNA (Figure 3B). The induction of TF gene transcription, however, was clearly lower when monocytes were incubated with PEGylated ORMOSIL-NPs.

The assay of TF activity in cell lysates confirmed the RT-PCR data. Monocytes treated with SAS-, PLGA- and SUV-NPs showed very little PCA, whereas monocytes incubated with ORMOSIL-NPs displayed a TF activity proportional to the concentration of the NPs (Figure 4). However, there was a striking difference between non-PEGylated and PEGylated ORMOSIL-NPs, the latter being much less effective in inducing monocyte TF activity (Figure 4).

Association of NPs to monocytes

Monocytes were incubated with a fluorescent-labeled version of our NP panel, with the exception of SAS. ORMOSIL-NPs were covalently labeled with cyanine IR775-Si, PLGA-NPs were loaded with fluorescein and SUV doped with PE-DPPC. Cells were incubated for 20 h with NPs, washed and analyzed by flow cytofluorimetry (Figure 5A). Results show that all tested non-PEGylated NPs bound to monocytes in a saturable way. At a concentration of 100 µg/ml, all NPs gave maximal cell binding. The binding curve of bare ORMOSIL-NPs fits with the dose–response of TF induction. Association of NPs to monocytes was not significantly reduced by PEGylation in the cases of PLGA- and SUV-NPs. However, PEGylated ORMOSIL-NPs were poorly captured compared with non-PEGylated NPs.

Nanoparticle capture by monocytes was evident after 4 h with the same pattern observed after 20 h, but was reduced by 60% (not shown).

Confocal microscopy analysis (Figure 5B) documented that all studied NPs are distributed within the monocyte cytoplasm in a punctuated fashion, compatible with their presence in endocytic/lysosomal vesicles. This suggests that

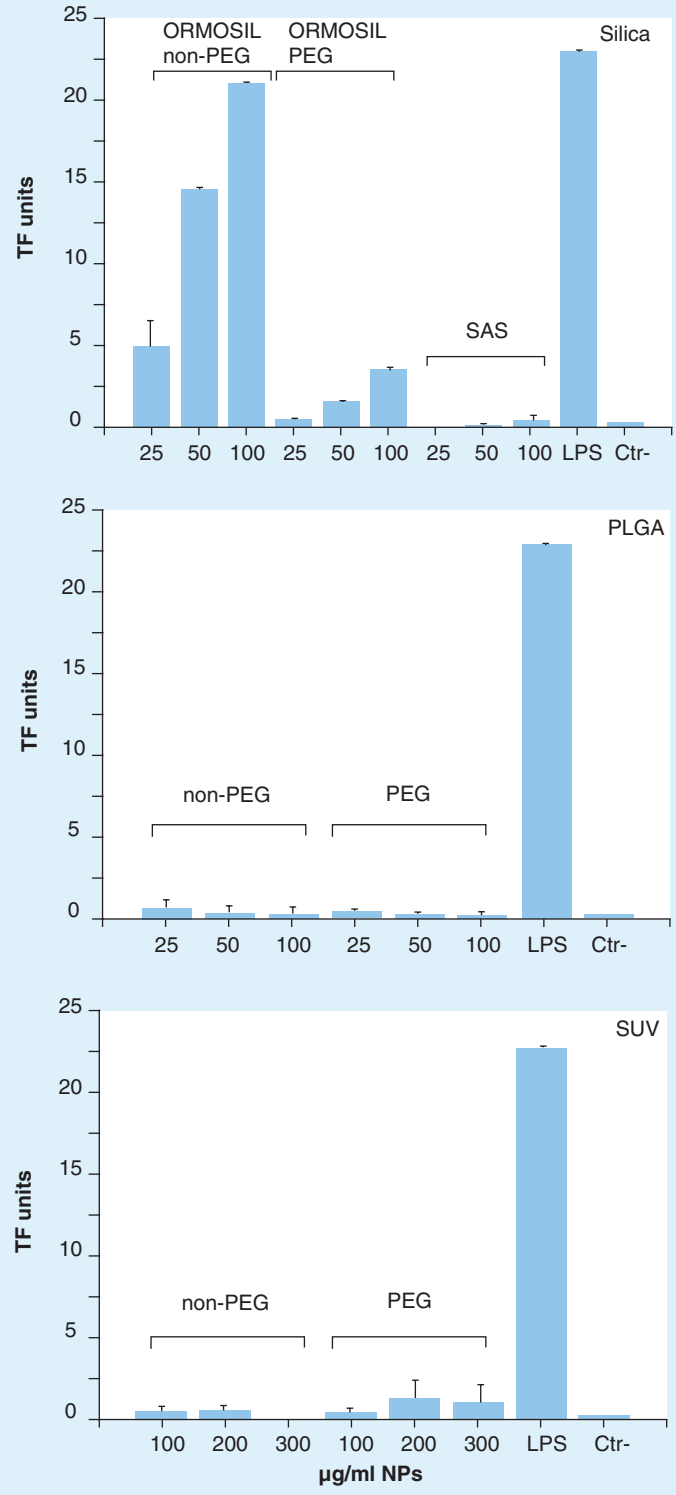

Figure 4. Tissue factor-dependent procoagulant activity of total lysates from nanoparticle-treated monocytes. Monocytes were treated for 20 h with different doses of the indicated NPs, scraped and lysed by three freeze–thaw cycles. Lysed cells were mixed with platelet-poor plasma in ratio of 1:1 and $CaCl_2$, and incubated at 37°C. The coagulation time of platelet-poor plasma was chronometrically determined and compared with a calibration curve obtained with defined amounts of recombinant TF. Cells incubated with 3000 EU/ml of lipopolysaccharide, were used as positive controls. Data, expressed as TF units, are the means of three independents experiments run in triplicate ± SE.
NP: Nanoparticle; ORMOSIL: Organically modified silica; PEG: Polyethylene glycol; PLGA: Poly(lactic-co-glycolic acid); SUV: Small unilamellar vesicle; TF: Tissue factor.

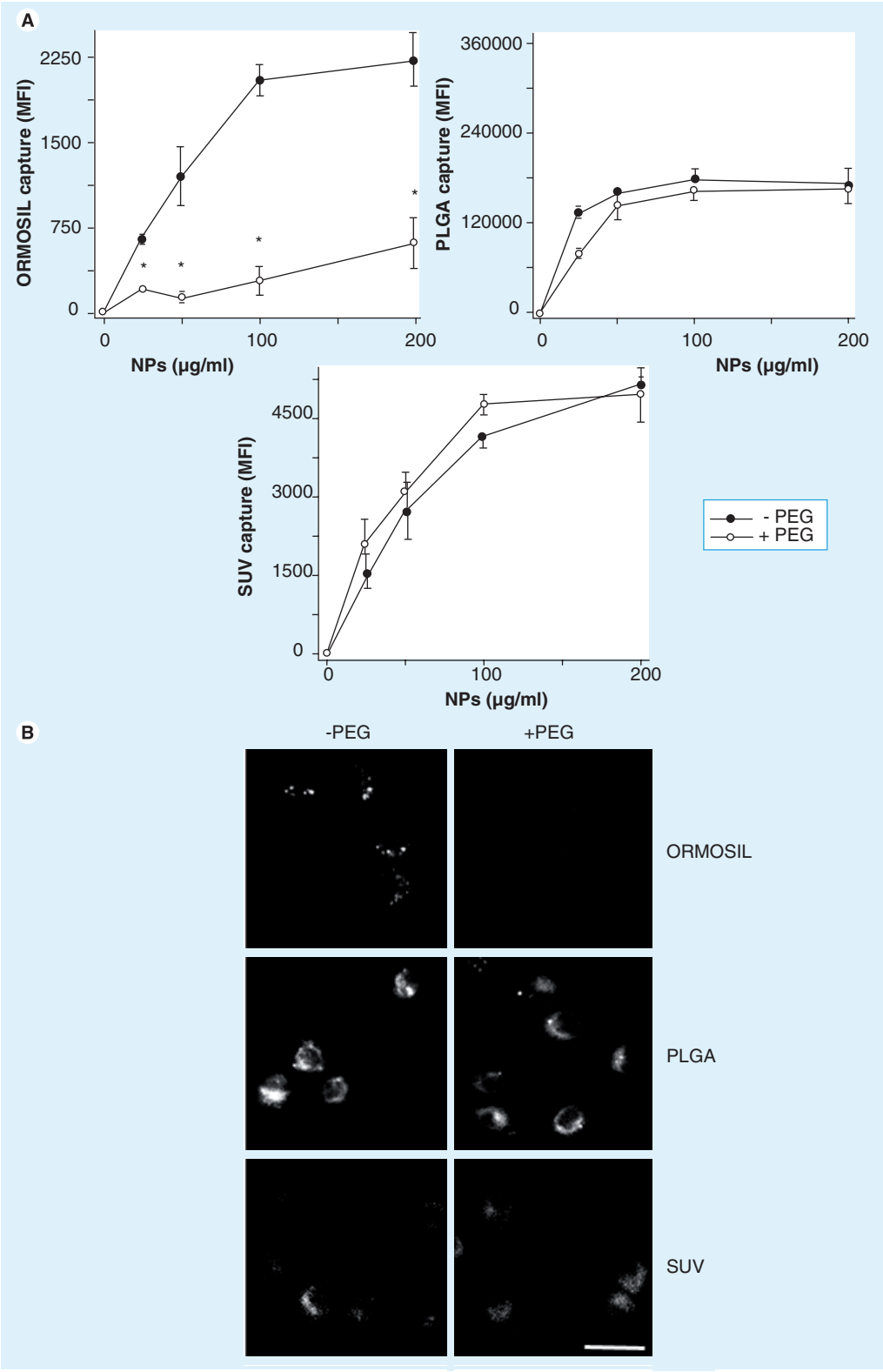

Figure 5. Association of bare and PEGylated nanoparticles to monocytes.
(A) Dose-dependent NP uptake by monocytes treated with different concentrations of PEGylated or non-PEGylated NPs for 20 h at 37°C. Uptake is expressed as MFI determined by cytofluorimetry. Significance of differences of PEGylated with respect to non-PEGylated NPs are indicated by *($p < 0.05$). **(B)** Confocal microscopy pictures showing the intracellular location of NPs after incubation with monocytes as above. Scale bar: 30 µm.
MFI: Mean fluorescence intensity; NP: Nanoparticle; ORMOSIL: Organically modified silica; PEG: Polyethylene glycol; PLGA: Poly(lactic-co-glycolic acid); SUV: Small unilamellar vesicle.

NPs are actively captured by cells and are therefore sequestered intracytoplasmically. PEGylated ORMOSIL-NPs gave a negligible signal, in agreement with flow cytometry data.

Interaction of NPs with HUVECs & platelets

Endothelial cells and platelets are major players in the coagulation process and in the formation of thrombi. In HUVECs, all tested NPs, including non-PEGylated and PEGylated ORMOSIL, had no appreciable effect of TF gene transcription (not shown). Consistently, none of the tested NPs caused an appreciable increase of cell PCA (TF activity <0.1 U/10^5 cells; n = 3; NPs = 200 µg/ml). Similarly, incubation of HUVECs with NPs did not increase the expression of E-selectin (Figure 6A), nor that of other endothelial cell activation markers (i.e., CD31, CD106 and CD54; <1% compared

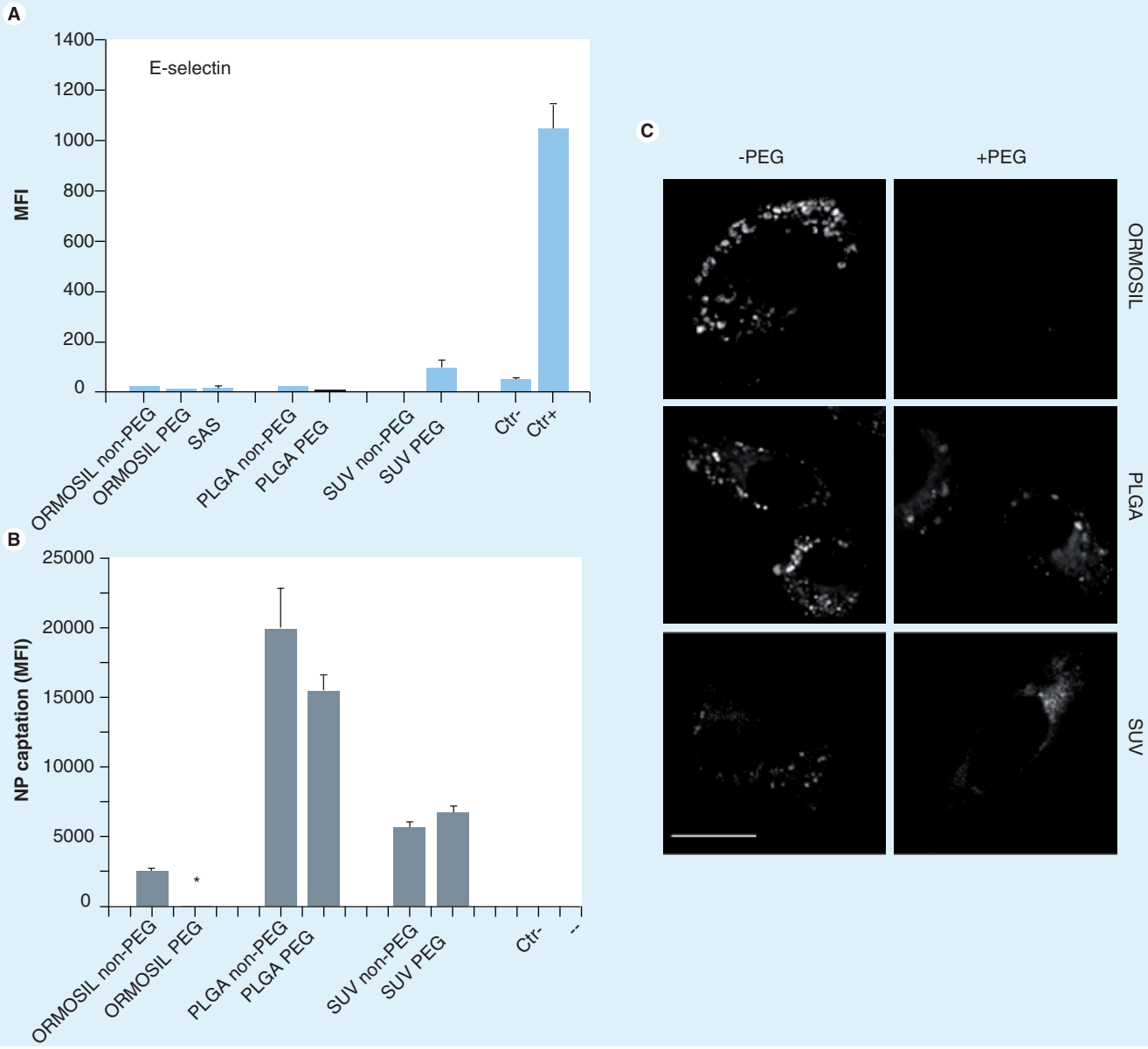

Figure 6. Binding of nanoparticles with human umbilical vein endothelial cells. (A) Expression of E-selectin on human umbilical vein endothelial cells, incubated with 50 µg/ml of the different NPs for 20 h. Samples incubated with E-selectin antibody were fixed in paraformaldehyde and data were acquired with cytofluorimetry. TNF-α treatment (20 ng/ml) was used as positive control. **(B)** Cytofluorimetric histograms showing the MFI of HUVECs treated with NPs. Significance of differences of PEGylated with respect to non-PEGylated NPs are indicated by *($p < 0.05$). **(C)** Confocal microscopy images showing the intracellular distribution of NPs in HUVECs treated with 50 µg/ml of the different NPs for 20 h. Scale bar: 100 µm.
Ctr: Control; MFI: Mean fluorescence intensity; NP: Nanoparticle; ORMOSIL: Organically modified silica; PEG: Polyethylene glycol; PLGA: Poly(lactic-co-glycolic acid); SAS: Synthetic amorphous silica; SUV: Small unilamellar vesicle.

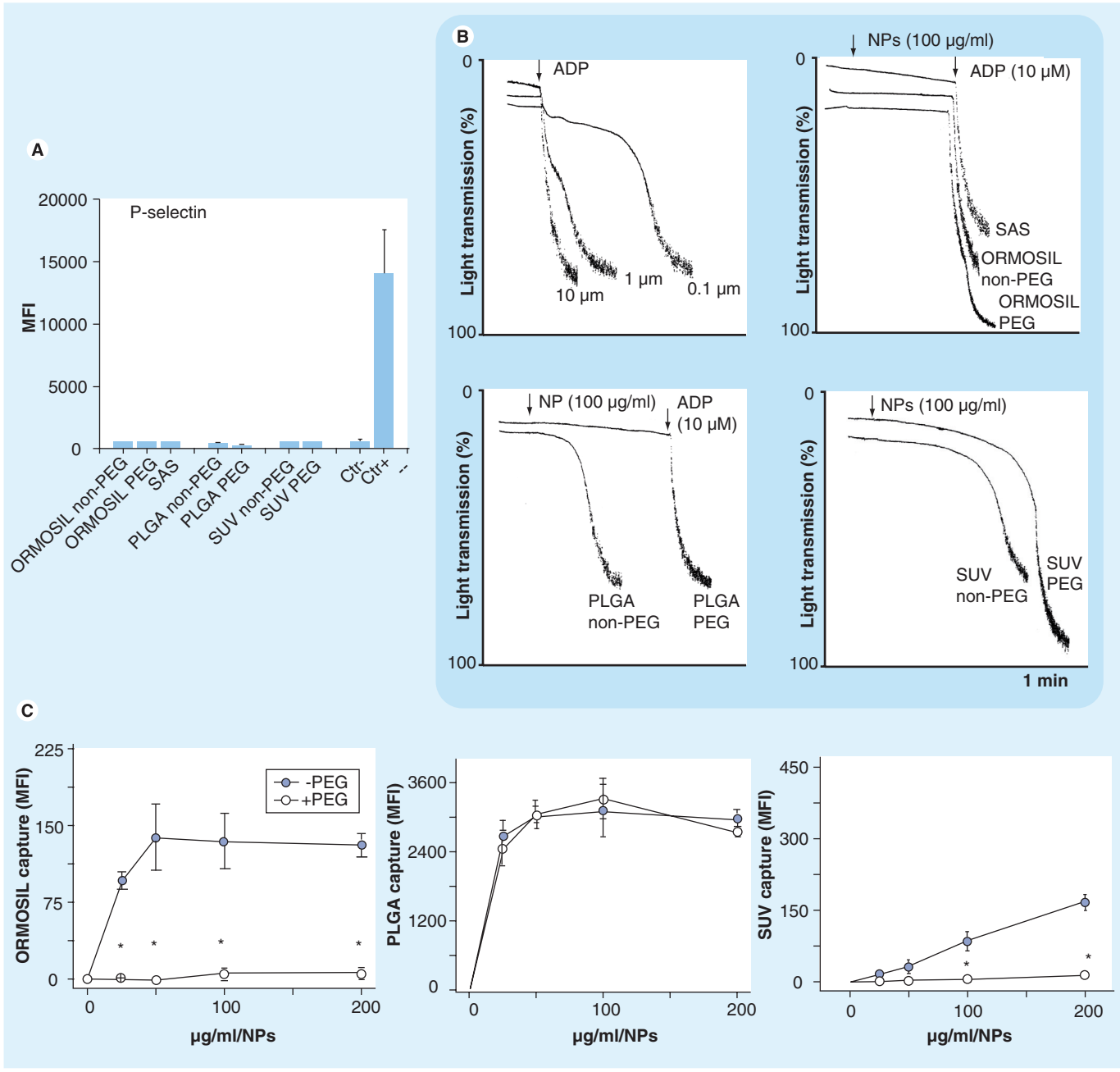

Figure 7. Effects of nanoparticles on platelets. (A) Expression of P-selectin on human platelets incubated with 50 µg/ml of the different NPs in saline solution for 10 min at 37°C; a mixture of different stimuli (α-THR, 1 U/ml, I-BOP 1 M and ADP 10 µM) was used as a positive control. Samples incubated with P-selectin antibody were fixed in paraformaldehyde and data were acquired with citofluorimetry. **(B)** Representative tracings of platelet aggregation induced by ADP or by different nanoparticles. The addition times of agonists are indicated by the arrows. **(C)** Dose-dependent NP uptake of platelets treated with non-PEGylated (-PEG) or PEGylated (+PEG) ORMOSIL, PLGA and SUV. Significance of values with respect to non-PEGylated NPs effects are indicated by *($p < 0.05$).
Ctr: Control; MFI: Mean fluorescence intensity; NP: Nanoparticle; ORMOSIL: Organically modified silica; PEG: Polyethylene glycol; PLGA: Poly(lactic-co-glycolic acid); SAS: Synthetic amorphous silica; SUV: Small unilamellar vesicle.

with cells incubated with TNF-α). Flow cytometry experiments and confocal microscopy analysis performed with labeled NPs (Figure 6 B & C) confirmed that, similar to that found in monocytes, PLGA- and SUV-NPs were endocytosed by endothelial cells, regardless of their PEGylation state, while PEGylation of ORMOSIL-NPs resulted in virtually a complete reduction of NP cell association and engulfment. NPs binding to HUVECs were evident after incubation for 2–4 h with a similar pattern, but its intensity was approximately 20–30% of that observed after 20 h incubation (not shown).

To evaluate the effect of NPs on platelets, they were incubated with PRP and the expression of P-selectin (CD62b) was compared with that induced by a mixture of typical platelet agonists used as positive controls (α-Thr, I-BOP and ADP). Figure 7A shows that CD62b expression was not increased by any NPs, indicating a lack of platelet activation.

Platelet aggregation in suspension and under stirring, a more physiological way to test platelet activation, was also performed to asses NP prothrombotic activity. Turbidimetric analysis (Figure 7B) showed that SAS-NPs, as well as bare and PEGylated ORMOSIL-NPs, did not induce a significant platelet aggregation effect, even when compared with suboptimal ADP (0.1 µM) stimulation, in agreement with CD62b upregulation analysis. Interestingly however, PLGA-NPs were shown to aggregate platelets in the bare version, while PEGylation abolished such activity. Bare SUVs showed a weak platelet aggregating effect, further diminished by PEGylation.

Flow cytometry data (Figure 7C) revealed that all NPs can rapidly associate with platelets. Prolonged incubations could not be performed owing to platelet instability. In agreement with data obtained with monocytes and HUVECs, PEGylation scarcely affected the PLGA-NPs association to platelets, while SUV- and ORMOSIL-NPs platelet binding was inhibited by PEG coating. Binding of NPs to platelets was saturable and reached its maximum at the concentration of approximately 50 µg/ml for bare ORMOSIL-NPs and bare or PEGylated-PLGA-NPs. Bare SUV binding was less efficient and did not saturate at concentrations up to 200 µg/ml.

Confocal microscopy analysis could not discriminate the distribution of NPs in the platelet structure owing to the small dimension of these structures (not shown).

Discussion

Nanoparticles used for the specific delivery of drugs to selected organs or tumors must be introduced into the bloodstream. The results obtained here emphasize that blood coagulation is a major difficulty in designing NPs for medical use. The surface of NPs may activate the coagulation cascade within minutes by directly interacting with factor XII (Hageman factor). This is the first step of the so-called intrinsic pathway, which is normally initiated by collagen after endothelial damage, or by negatively charged surfaces, such as glass. Alternatively, NPs may induce blood monocytes, endothelial cells and platelets to upregulate TF, a membrane protein that initiates the extrinsic coagulation cascade. The extent to which NPs activate the coagulation cascade relies, in the end, on the properties of their surface and namely on their ability to bind proteins and other molecules present in the blood, in solution or on cells. Indeed, NPs are particularly prone to activate undesired surface interaction with host components owing to their extremely high area:volume ratio. Even a material that is inert in bulk form may become active at the nanoscopic level [40]. Moreover, direct binding of NPs to specific cellular receptors has been well documented in alveolar macrophages. In these cells, MARCO scavenger receptors mediate the cytotoxic and proinflammatory effects of silica and other NPs [41,42].

In this study, we proved that immediate activation of the intrinsic coagulation cascade via factor XII is the first threat concerning NP biocompatibility. We actually observed that SAS-NPs are very active in inducing coagulation by the contact pathway. Since SAS-NPs did not induce TF expression in monocytes and endothelial cells, it is conceivable that their efficacy to trigger a rapid blood–plasma coagulation is determined by their high superficial negative charge due to the deprotonated surface silanol group (pKa ≈ 3). Indeed, SAS-NPs may be regarded as highly porous nano-beads made of glass – a material known to effectively bind the Hageman factor. Experiments performed with deficient plasma confirmed that factor XII is responsible for coagulation induced by SAS-NPs. This observation raises further concern on the potentially toxic effects of SAS-NPs.

On the contrary, ORMOSIL-NPs prepared from vinyltriethoxysilane did not coagulate blood and had a minor effect on plasma clotting. This suggests that contact activation, although present, is poor, possibly because ORMOSIL-NPs, in contrast to inorganic NPs, have a lower negative superficial charge, as evidenced by the lower zeta-potential value (-6.2 mV) for these NPs compared with SAS-NPs (-25.9 mV). In addition, ORMOSIL-NPs may also display superficial vinyl groups conferring a reduced polarity to the NP surface.

Most important, we demonstrated that this residual PCA was totally eliminated by PEGylation. In fact, highly PEGylated ORMOSIL-NPs are devoid of detectable plasma coagulation, similar to PEGylated SUV- and PLGA-NPs. This indicated that PEGylated ORMOSIL-NPs do not interact with soluble procoagulant factors and, in this respect, perform similarly to other PEGylated NPs.

As previously mentioned, blood coagulation may also be cell mediated. In this case, some cells within the bloodstream are activated by a given agonist and as a result they upregulate the protein TF, which, expressed on the cell surface, initiates an alternative coagulation cascade leading to fibrin deposition. When this second mechanism of plasma coagulation was investigated, ORMOSIL-NPs were found to be paradoxically more active than SAS-NPs in inducing TF in monocytes. RT-PCR clearly showed that ORMOSIL-NPs increased transcription of the TF gene in monocytes, while PLGA and liposome NPs were all inactive. We interpret these data assuming that the introduction of nonpolar vinyl groups on ORMOSIL-NPs, while diminishing their binding to the initiators of the intrinsic coagulation cascade, at the same time favor the adsorption of opsonines through hydrophobic interactions, mediating monocyte binding and activation. In fact, as evidenced by Dutta *et al.*, the pattern of proteins adsorbed by given NPs may influence their cellular targeting and uptake [43]. Although in the future the use of different organic derivatives of silicon may diminish the procoagulation activity of naked ORMOSIL-NPs, it should be noted that, once again, PEGylation of ORMOSIL-NPs strongly decreased their ability to induce a TF-dependent PCA in monocytes. Flow cytometry and confocal microscopy analysis indicated that surface PEGylation decreased monocyte TF upregulation by ORMOSIL-NPs because it hampered NP phagocytosis, consistent with data obtained using differentiated macrophages [32]. Additional evidence of the good biocompatibility of PEG-coated ORMOSIL-NPs are provided in this study. In fact, PEGylated ORMOSIL-NPs did not associate and did not activate endothelial cells and platelets. The superior stealth properties of our highly PEGylated ORMOSIL-NPs are evident if we analyze the uptake of other NPs to the same cellular elements. The decrease in cell uptake of PEGylated liposomes and PLGA-NPs compared with non-PEGylated NPs is in fact partial or, in some cases, nonsignificant. Hence, PEG density appears to be a crucial aspect to avoid undesired NP interaction with cells; in liposomes and PLGA-NPs, a PEG content higher than 8% may cause stability problems [Kos J, Scheglmann D, Unpublished Observations]. By contrast, ORMOSIL-NPs, owing to their special cosynthesis of organic-Si monomers with PEG silane derivatives, and likely because of the high stability of the covalent network of the matrix, can reach values that are much higher (30–67%, depending on the synthesis condition and on the NP size) [32].

Conclusion

Silica NPs, either made from SAS or ORMOSIL, showed important PCA, which seriously threatens their use for nanomedicine and drug-delivery applications. Interestingly, PCA appears to follow a different mechanism, depending on the material from which the NPs are made. In fact, SAS-NPs activate contact coagulation (factor XII dependent) but not TF transcription in monocytes, while ORMOSIL-NPs induce TF-dependent coagulation more efficiently. However, on the whole, our data indicate that a thick superficial packing of PEG, reaching values of approximately 37% w/w for ORMOSIL-NPs with a diameter of 50 nm, results in nanosystems with a PCA similar, if not lower, than that of typical biocompatible organic NPs based on PLGA and liposomes. Conversely, PEGylated ORMOSIL-NPs are endowed with much improved stealth properties.Thus, highly PEGylated ORMOSIL-NPs might be considered the minimal structural base for the development of biocompatible functionalized nanotheragnostics.

Future perspective

Improved hemocompatibility, together with the great versatility of PEGylated ORMOSIL-NPs, could allow further development of more complex engineered nanocarriers or 'nanomachines'. Incorporation of functional chemical groups into a fraction of superficial PEG coating chains may be useful to add cell-specific ligands for diagnosis and therapy. At present, we are testing the possibility of generating PEGylated ORMOSIL-NPs containing photosensitizers covalently linked to the silica matrix in cellular and animal models. We will subsequently improve these NPs by superficial derivatization with cancer-specific ligands (EGF, folic acid and humanized antiprostate-specific membrane antigen antibodies) for a more efficient photodynamic therapy approach.

Acknowledgements

We thank the Centro Trasfusionale of the Hospital of Padua (ULSS 16) for providing buffy coats, Fabio Di Lisa and Giovanni Abatangelo for blood sampling, and Renzo Deana for the use of an aggregometer. We are grateful to Enrico Rampazzo from the Dipartimento di Chimica 'G. Ciamician' of the University of Bologna for zeta-potential measurements.

Financial & competing interests disclosure

The research leading to these results has received funding from the European Community's Seventh Framework Programme (FP7/2007–2013) under grant agreement no. 201031 NANOPHOTO. The authors have no other relevant affiliations or financial involvement with any organization or entity with a financial interest in or financial conflict with the subject matter or materials discussed in the manuscript apart from those disclosed.

No writing assistance was utilized in the production of this manuscript.

Ethical conduct of research

The authors state that they have obtained appropriate institutional review board approval or have followed the principles outlined in the Declaration of Helsinki for all human or animal experimental investigations. In addition, for investigations involving human subjects, informed consent has been obtained from the participants involved.

Executive summary

- Organically modified silica nanoparticles (NPs; 45–50 nm diameter) were synthesized using vinyltriethoxysilane in non-PEGylated or highly PEGylated (37% w/w) forms using a one-pot procedure recently developed by us, envisaging the polymerization of lipophylic organosilane derivatives in the hydrophobic core of detergent micelles and the simultaneous covalent grafting of polyethylenglycol to the silica matrix.
- Direct and cell-mediated clot-promoting properties of naked and highly PEGylated organically modified silica (ORMOSIL)-NPs were compared with those of synthetic amorphous silica-NPs, fully inorganic structures largely used in industry, and of poly(lactic-co-glycolic acid) (PLGA) and liposomal NPs, two formulations already approved for the use in humans, produced by us in naked or in PEGylated forms.
- When added to blood or plasma, synthetic amorphous silica-NPs markedly accelerated clot formation in a factor XII-dependent way, while ORMOSIL-NPs had a much weaker activity, detectable only in plasma, which was totally abolished by surface PEGylation.
- After prolonged incubation, bare ORMOSIL-NPs, in contrast to other NPs, induced tissue factor mRNA and activity in monocytes. This effect, however, was strongly reduced by PEGylation.
- None of the NPs induced tissue factor in endothelial cells. Moreover, no tested NPs induced the expression of activation markers in platelets and endothelial cells. Some significant platelet aggregation was induced by bare PLGA, but not by the other NPs.
- While PEGylated PLGA and PEGylated liposomal NPs associate to monocytes, endothelial cells and platelets similar to their naked versions, PEGylation of ORMOSIL-NPs resulted in more than 88% inhibition of the binding to these cells.
- The dense PEG-coating achievable with our synthesis procedure makes organically modified silica a promising constructing material to design stealth NPs for selective drug targeting, such as photodynamic therapy or other innovative therapies, devoid of procoagulating effects, which is a major drawback of any medical devices in contact with the blood.
- Screening of procoagulant activity is a valuable approach to test NP biocompatibility.

Bibliography

1 Liang XJ, Chen C, Zhao Y, Jia L, Wang PC: Biopharmaceutics and therapeutic potential of engineered nanomaterials. *Curr. Drug Metab.* 9(8), 697–709 (2008).

2 Liu Y, Miyoshi H, Nakamura M: Nanomedicine for drug delivery and imaging: a promising avenue for cancer therapy and diagnosis using targeted functional nanoparticles. *Int. J. Cancer.* 120(12), 2527–2537 (2007).

3 Bazile D, Prud'homme C, Bassoullet MT, Marlard M, Spenlehauer G, Veillard M: Stealth Me.PEG–PLA nanoparticles avoid uptake by the mononuclear phagocytes system. *J. Pharm. Sci.* 84(4), 493–498 (1995).

4 Hoet PH, Bruske-Hohlfeld I, Salata OV: Nanoparticles – known and unknown health risks. *J. Nanobiotechnol.* 2(1), 12 (2004).

5 De Jong WH, Borm PJ: Drug delivery and nanoparticles: applications and hazards. *Int. J. Nanomed.* 3(2), 133–149 (2008).

6 Schmaier AH: Assembly, activation, and physiologic influence of the plasma kallikrein/kinin system. *Int. Immunopharmacol.* 8(2), 161–165 (2008).

7 Semeraro N, Colucci M: Tissue factor in health and disease. *Thromb. Haemost.* 78(1), 759–764 (1997).

8 Borm PJ, Kreyling W: Toxicological hazards of inhaled nanoparticles – potential implications for drug delivery. *J. Nanosci. Nanotechnol.* 4(5), 521–531 (2004).

9 Oberdorster G, Oberdorster E, Oberdorster J: Nanotoxicology: an emerging discipline evolving from studies of ultrafine particles. *Environ. Health Perspect.* 113(7), 823–839 (2005).

10 Khandoga A, Stampfl A, Takenaka S *et al.*: Ultrafine particles exert prothrombotic but not inflammatory effects on the hepatic microcirculation in healthy mice *in vivo*. *Circulation* 109(10), 1320–1325 (2004).

11 Radomski A, Jurasz P, Alonso-Escolano D *et al.*: Nanoparticle-induced platelet aggregation and vascular thrombosis. *Br. J. Pharmacol.* 146(6), 882–893 (2005).

12 Gorbet MB, Sefton MV: Biomaterial-associated thrombosis: roles of coagulation factors, complement, platelets and leukocytes. *Biomaterials* 25(26), 5681–5703 (2004).

13 Peracchia MT, Fattal E, Desmaele D *et al.*: Stealth PEGylated polycyanoacrylate nanoparticles for intravenous administration and splenic targeting. *J. Control. Release* 60(1), 121–128 (1999).

14 Li SD, Huang L: Nanoparticles evading the reticuloendothelial system: role of the supported bilayer. *Biochim. Biophys. Acta.* 1788(10), 2259–2266 (2009).

15 Barbe C, Bartlett J, Kong LG *et al.*: Silica particles: a novel drug-delivery system. *Adv. Mater.* 16, 1959–1966 (2004).

16 Slowing II, Trewyn BG, Lin VS: Mesoporous silica nanoparticles for intracellular delivery of membrane-impermeable proteins. *J. Am. Chem. Soc.* 129(28), 8845–8849 (2007).

17 Barik TK, Sahu B, Swain V: Nanosilica – from medicine to pest control. *Parasitol. Res.* 103(2), 253–258 (2008).

18 Bharali DJ, Klejbor I, Stachowiak EK *et al.*: Organically modified silica nanoparticles: a nonviral vector for *in vivo* gene delivery and expression in the brain. *Proc. Natl Acad. Sci. USA* 102(32), 11539–11544 (2005).

19 Chan Z, Ai'mei L, Xiao Z, Miao F, Juan H, Hongbin Z: Microstructure and properties of ORMOSIL comprising methyl, vinyl, and g-glycidoxypropyl-substituted silica. *Optical Materials* 29, 1543–1547 (2007).

20 Ohulchanskyy TY, Roy I, Goswami LN *et al.*: Organically modified silica nanoparticles with covalently incorporated photosensitizer for photodynamic therapy of cancer. *Nano. Lett.* 7(9), 2835–2842 (2007).

21 Kumar R, Roy I, Ohulchanskyy TY *et al.*: Covalently dye-linked, surface-controlled, and bioconjugated organically modified silica nanoparticles as targeted probes for optical imaging. *ACS Nano.* 2(3), 449–456 (2008).

22 Reuzel PG, Bruijntjes JP, Feron VJ, Woutersen RA: Subchronic inhalation toxicity of amorphous silicas and quartz dust in rats. *Food Chem.Toxicol.* 29(5), 341–354 (1991).

23 Hamilton RF Jr, Thakur SA, Holian A: Silica binding and toxicity in alveolar macrophages. *Free Radic. Biol. Med.* 44(7), 1246–1258 (2008).

24 Cho WS, Choi M, Han BS *et al.*: Inflammatory mediators induced by intratracheal instillation of ultrafine amorphous silica particles. *Toxicol. Lett.* 175(1–3), 24–33 (2007).

25 Chang JS, Chang KL, Hwang DF, Kong ZL: *In vitro* cytotoxicitiy of silica nanoparticles at high concentrations strongly depends on the metabolic activity type of the cell line. *Environ. Sci. Technol.* 41(6), 2064–2068 (2007).

26 Lin W, Huang YW, Zhou XD, Ma Y: *In vitro* toxicity of silica nanoparticles in human lung cancer cells. *Toxicol. Appl. Pharmacol.* 217(3), 252–259 (2006).

27 Park EJ, Park K: Oxidative stress and proinflammatory responses induced by silica nanoparticles *in vivo* and *in vitro. Toxicol. Lett.* 184(1), 18–25 (2009).

28 Kaewamatawong T, Shimada A, Okajima M *et al.*: Acute and subacute pulmonary toxicity of low dose of ultrafine colloidal silica particles in mice after intratracheal instillation. *Toxicol. Pathol.* 34(7), 958–965 (2006).

29 Cho M, Cho WS, Choi M *et al.*: The impact of size on tissue distribution and elimination by single intravenous injection of silica nanoparticles. *Toxicol. Lett.* 189(3), 177–183 (2009).

30 Roy I, Ohulchanskyy TY, Pudavar HE *et al.*: Ceramic-based nanoparticles entrapping water-insoluble photosensitizing anticancer drugs: a novel drug-carrier system for photodynamic therapy. *J. Am. Chem. Soc.* 125(26), 7860–7865 (2003).

31 Roy I, Ohulchanskyy TY, Bharali DJ *et al.*: Optical tracking of organically modified silica nanoparticles as DNA carriers: a nonviral, nanomedicine approach for gene delivery. *Proc. Natl Acad. Sci. USA* 102(2), 279–284 (2005).

32 Rio-Echevarria IM, Selvestrel F, Segat D *et al.*: Highly PEGylated silica nanoparticles: "ready to use" stealth functional nanocarriers. *J. Mater. Chem.* 20, 2780–2787 (2010).

33 Roskos KV, Maskiewicz R: Degradable controlled release systems useful for protein delivery. *Pharm. Biotechnol.* 10, 45–92 (1997).

34 Huwyler J, Drewe J, Krahenbuhl S: Tumor targeting using liposomal antineoplastic drugs. *Int. J. Nanomed.* 3(1), 21–29 (2008).

35 Gabizon AA, Shmeeda H, Zalipsky S: Pros and cons of the liposome platform in cancer drug targeting. *J. Liposome Res.* 16(3), 175–183 (2006).

36 Kocbek P, Obermajer N, Cegnar M, Kos J, Kristl J: Targeting cancer cells using PLGA nanoparticles surface modified with monoclonal antibody. *J. Control. Release* 120(1–2), 18–26 (2007).

37 Semeraro N, Biondi A, Lorenzet R, Locati D, Mantovani A, Donati MB: Direct induction of tissue factor synthesis by endotoxin in human macrophages from diverse anatomical sites. *Immunology* 50(4), 529–535 (1983).

38 Koziara JM, Oh JJ, Akers WS, Ferraris SP, Mumper RJ: Blood compatibility of cetyl alcohol/polysorbate-based nanoparticles. *Pharm. Res.* 22(11), 1821–1828 (2005).

39 Kornalik F, Blomback B: Prothrombin activation induced by ecarin – a prothrombin converting enzyme from *Echis carinatus* venom. *Thromb. Res.* 6(1), 57–63 (1975).

40 Nel A, Xia T, Madler L, Li N: Toxic potential of materials at the nanolevel. *Science* 311(5761), 622–627 (2006).

41 Hamilton RF Jr, Thakur SA, Mayfair JK, Holian A: MARCO mediates silica uptake and toxicity in alveolar macrophages from C57BL/6 mice. *J. Biol. Chem.* 281(45), 34218–34226 (2006).

42 Thakur SA, Hamilton RF Jr, Pikkarainen T, Holian A: Differential binding of inorganic particles to MARCO. *Toxicol. Sci.* 107(1), 238–246 (2009).

43 Dutta D, Sundaram SK, Teeguarden JG *et al.*: Adsorbed proteins influence the biological activity and molecular targeting of nanomaterials. *Toxicol. Sci.* 100(1), 303–315 (2007).